Proceedings of GPPS Forum 18
Global Power and Propulsion Society
Montreal, 7th-9th May 2018
www.gpps.global

GPPS-NA-2018-0097

A Comparison of Strategies for Efficient Core Engine Optimization with Coupled Subsystems

Simon Extra
Brandenburg University of Technology
extra@b-tu.de
03046 Cottbus, Brandenburg, Germany

Michael Lockan
Brandenburg University of Technology
michael.lockan@b-tu.de
03046 Cottbus, Brandenburg, Germany

Dieter Bestle
Brandenburg University of Technology
bestle@b-tu.de
03046 Cottbus, Brandenburg, Germany

Peter Flassig
Rolls-Royce Deutschland Ltd & Co KG
Peter.Flassig@Rolls-Royce.com
15827 Blankenfelde-Mahlow, Brandenburg, Germany

ABSTRACT
The present paper compares four different optimization strategies for decoupled optimization in the context of preliminary core engine design for aero engines. An optimization with the AAO (All-At-Once) approach is performed as a baseline and compared against the performance and results of three cascaded optimization strategies: CO (Collaborative Optimization), BLISS 2000 (Bi-Level Integrated System Synthesis) and ISOC (Interface Segmentation Optimization Concept). The optimization problem is based on a thermodynamic core engine model representing an industrial application example. The results are assessed with respect to typical requirements for multidisciplinary core engine design. The impact of the used optimization strategy on the performance of the optimization concept is investigated and discussed.

INTRODUCTION
The current state of the art of aero engine preliminary design is based on decoupled component optimization, where the interface parameters between components are defined very early in the development cycle using low-fidelity performance calculations. These use either simple thermodynamic equations or scaled performance estimates from previously executed engine projects (Kupijai, 2014) which are not necessarily optimal. Based on these fixed interfaces, each component is then optimized by a team of experts with little opportunity to adapt the interface quantities. This may yield locally optimal results for the components which, however, are heavily constrained by the fixed interfaces. To allow for an improved overall design of the core engine, a coupled approach with three subsystem processes and adaptable interface quantities is proposed. These three processes for compressor (C), combustor (B) and turbine (T) are combined with a global optimizer seeking for overall optimized performance while keeping required constraints within their limits. Depending on the optimization structure, the global optimizer influences only global design and interface variables, while the subtasks account for local component design variables. Through this, the performance of both the components and their interactions are taken into consideration.

THERMODYNAMIC MODEL FOR DECOUPLED CORE ENGINE OPTIMIZATION
A thermodynamic representation of the core engine of a typical two-shaft aero engine is used as a fast way to evaluate an industrial application example. It allows for a statistical investigation of the various coupling strategies based on a large number of function evaluations. Nonetheless the system behavior is represented truthfully enough and the findings of this paper may be applied with only little changes to a more sophisticated preliminary core engine optimization process with more detailed component representations as used by Extra et al. (2017). The structure of the thermodynamic process is based on Bräunling (2009) as shown in Fig. 1, where the core engine is divided into three coupled subsystems representing compressor, combustor and turbine. A more complex, high-fidelity simulation of the coupled subsystems may require interfaces of higher dimensionality, but the overall structure of this coupled core engine design process will be identical.

We assume that there is a set of shared design variables containing variables which are used by at least two components, e.g. gas path cross sections A_3, A_4 and total

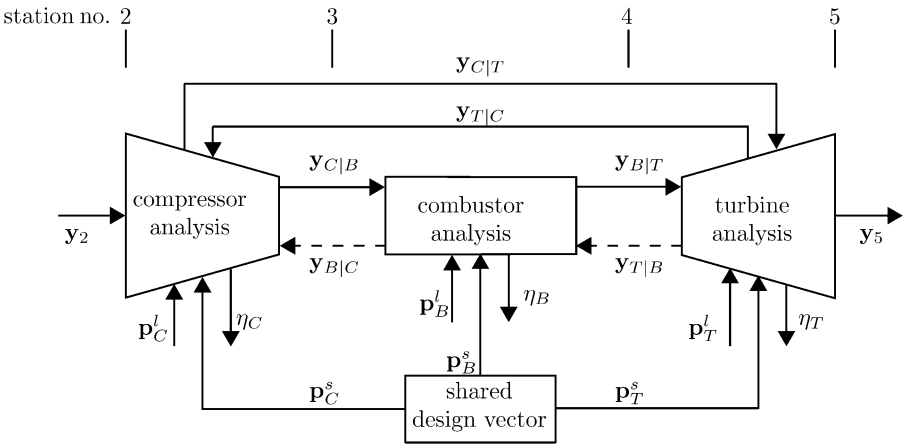

Figure 1 Coupled core engine design problem

temperature T_{t4} at the combustor exit station summarized as

$$\mathbf{p}^s = [A_3, A_4, T_{t4}]^T. \tag{1}$$

The inlet of the compressor module is defined by inlet mass flow $\dot{m}_2$, inlet total pressure p_{t2} and inlet total temperature T_{t2} which are assumed to be fixed and summarized as

$$\mathbf{y}_2 = [\dot{m}_2, p_{t2}, T_{t2}]^T. \tag{2}$$

Each component is determined by some of the shared variables (1) and local design variables $\mathbf{p}^l$. For the compressor, the local variable is chosen to be the fraction α of the bleed air offtake for turbine cooling and the relevant shared variable is the compressor exit flow area A_3 summarized as

$$\mathbf{p}_C = \left[\mathbf{p}_C^{l^T}, \mathbf{p}_C^{s^T}\right]^T \tag{3}$$

where

$$\mathbf{p}_C^l = [\alpha], \quad \mathbf{p}_C^s = [A_3]. \tag{4}$$

These values are used to calculate outputs by compressor analysis using basic thermodynamic equations. The resulting outputs of each component calculation are used either as coupling quantities and inputs to other components or as return values to be used as part of a global objective or constraint function. For the compressor, we define exit mass flow $\dot{m}_3$, total temperature at compressor exit T_{t3} and total pressure p_{t3} as interfaces to the combustor component and the bleed air mass flow $\dot{m}_z$ as interface provided to the turbine. They are summarized in coupling vectors

$$\mathbf{y}_{C|B} = [\dot{m}_3, T_{t3}, p_{t3}]^T, \ \mathbf{y}_{C|T} = [\dot{m}_z]. \tag{5}$$

The return value of the compressor component is its polytropic efficiency η_C calculated from the pressure ratio π_C, the ratio of specific heats κ as well as total inlet and outlet temperatures T_{t2} and T_{t3} as

$$\eta_C = \frac{\log\left(\pi_C^{(\kappa-1)/\kappa}\right)}{\log(T_{t3}/T_{t2})}. \tag{6}$$

The pressure ratio is defined through total pressures at inlet (p_{t2}) and outlet (p_{t3}).

The combustor module is coupled to the compressor through the coupling vector (5) being used as an input for the calculations. The local design variables for the combustor are the fuel-to-air-ratio β and the pressure ratio π_B over the combustor module. Shared variables are the inlet and outlet flow areas A_3, A_4 and the total temperature at combustor exit T_{t4} resulting in

$$\mathbf{p}_B = \left[\mathbf{p}_B^{l^T}, \mathbf{p}_B^{s^T}\right]^T \tag{7}$$

where

$$\mathbf{p}_B^l = [\beta, \pi_B]^T, \quad \mathbf{p}_B^s = [A_3, A_4, T_{t4}]^T. \tag{8}$$

The coupling $\mathbf{y}_{B|T}$ towards the turbine is again calculated from basic thermodynamic equations describing the behavior of the combustor. Results are the mass flow $\dot{m}_4$ and the total pressure p_{t4} defining coupling vector

$$\mathbf{y}_{B|T} = [\dot{m}_4, p_{t4}]^T. \tag{9}$$

In this example, we assume no upstream coupling $\mathbf{y}_{B|C}$ between combustor and compressor and $\mathbf{y}_{T|B}$ between turbine and combustor. The combustor efficiency η_B is calculated as relationship between the change in gas temperature achieved across the combustor for a given inlet mass flow $\dot{m}_3$ and the amount $\dot{m}_f$ of used fuel with a given specific heating value H_u as

$$\eta_B = \frac{\dot{m}_3}{\dot{m}_f} \frac{c_{ps}\left(T_{t4} - T_{ref}\right) - c_p\left(T_{t3} - T_{ref}\right)}{H_u - c_{ps}\left(T_{t4} - T_{ref}\right)} \tag{10}$$

where c_p and c_{ps} are specific heat capacities for compressed air and combustion exhaust gas relative to the reference temperature $T_{ref} = 298.15\text{K}$, respectively.

Finally the turbine is provided with input from the compressor as well as the combustor component denoted by coupling vectors $\mathbf{y}_{C|T}$ and $\mathbf{y}_{B|T}$. The coupling towards the compressor is expressed through the shaft power P provided by the turbine and driving the compressor:

$$\mathbf{y}_{T|C} = [P]. \tag{11}$$

The local design variable of the turbine is its pressure ratio π_T and shared variables are the turbine inlet flow area A_4 and total temperature at turbine inlet T_{t4}:

$$\mathbf{p}_T = \left[\mathbf{p}_T^{l^T}, \mathbf{p}_T^{s^T}\right]^T \tag{12}$$

where

$$\mathbf{p}_T^l = [\pi_T], \;\; \mathbf{p}_T^s = [A_4, T_{t4}]^T. \tag{13}$$

They are used as inputs for the calculation of turbine exit total temperature T_{t5} defining the turbine polytropic efficiency as

$$\eta_T = \frac{\log(T_{t5}/T_{t4})}{\log\left(\pi_T^{(\kappa_s-1)/\kappa_s}\right)} \tag{14}$$

where κ_s is the ratio of specific heats for the exhaust gas. Another result of the turbine analysis are the flow states at turbine exit, i.e., Mach number M_5, total temperature T_{t5} and total pressure p_{t5} summarized in turbine exit state

$$\mathbf{y}_5 = [M_5, T_{t5}, p_{t5}]^T \tag{15}$$

used to ensure coupling consistency towards the whole engine.

REFERENCE OPTIMIZATION STRATEGY

To establish a reference optimization problem and to motivate the use of a cascaded optimization scheme, All-At-Once (AAO) optimization is performed first. Here all design variables, local and shared ones, are directly varied by a single optimizer, Cramer et al. (1994). The subsystem equations are only used as analysis codes and do not incorporate any optimization on their own. This results in a simple structure with only one optimization algorithm and avoids problems regarding coupling coherence. This in turn leads directly to the downside of the approach in case of complex systems with a high number of design variables, if optimized at once. Convergence is hindered by the high-dimensional design space, and there is no possibility of influencing the interfaces directly.

The goal for this core engine optimization is the maximization of the simplified overall engine efficiency defined as product of the three component efficiencies (6), (10) and (14):

$$\eta = \eta_C \eta_B \eta_T. \tag{16}$$

Whilst deviating from a more common definition of core engine efficiency, it is very well suited for investigating decoupled optimization schemes. The AAO optimization problem then reads as

$$\max_{\mathbf{x}\in P} \eta \quad \text{where} \quad P = \left\{\mathbf{x} \in \mathbb{R}^7 \middle| \|\mathbf{y}_5 - \tilde{\mathbf{y}}_5\|_2 \le \varepsilon_T^l, \check{\mathbf{x}} \le \mathbf{x} \le \hat{\mathbf{x}}\right\}. \tag{17}$$

The overall design vector $\mathbf{x}$ contains the shared variables (1) as well as the local variables for each subsystem as described in the previous section. Turbine exit coupling (15) is considered as an inequality constraint enforcing consistency with prescribed values $\tilde{\mathbf{y}}_5$ within a tolerance ε_T^l.

POTENTIAL OPTIMIZATION STRATEGIES FOR SUBSYSTEM COUPLING

Three different existing cascaded optimization structures are shortly presented, investigated and compared to overcome the limitations imposed by the AAO approach. Whilst all are based on decomposition as described by Sobieszczanski-Sobieski (1984), there are differences in the subsystem goal definition, allocation of variables and use of constraints.

Collaborative Optimization (CO)

The first cascaded method is CO where a global optimizer handles shared design variables, goals for coupling states to be fulfilled by each subsystem optimization (Braun and Kroo, 1995), and goals for the component efficiencies. The global design vector then reads as

$$\mathbf{x}_g = \left[\mathbf{p}^{s^T}, \tilde{\mathbf{y}}_{C|B}^T, \tilde{\mathbf{y}}_{C|T}^T, \tilde{\mathbf{y}}_{B|T}^T, \tilde{\mathbf{y}}_{T|C}^T, \tilde{\eta}_C, \tilde{\eta}_B, \tilde{\eta}_T\right]^T. \tag{18}$$

The prescribed efficiency goals are used to calculate the overall engine efficiency as

$$\tilde{\eta} = \tilde{\eta}_C \tilde{\eta}_B \tilde{\eta}_T \tag{19}$$

similar to Eq. (16). According to Fig. 2, the goals are given to component optimization processes which have to achieve a consistent system state by minimizing errors f_i between component calculation results and prescribed goals. The fulfilment of these constraints is checked in the overall system optimization by comparing minimized errors f_i^* to user-defined tolerances ε_i:

$$\max_{\mathbf{x}_g\in P} \tilde{\eta} \text{ where } P = \left\{\mathbf{x}_g \in \mathbb{R}^{13} \middle| \begin{bmatrix} f_C^* \\ f_B^* \\ f_T^* \end{bmatrix} \le \begin{bmatrix} \varepsilon_C \\ \varepsilon_B \\ \varepsilon_T \end{bmatrix}, \check{\mathbf{x}}_g \le \mathbf{x}_g \le \hat{\mathbf{x}}_g \right\}. \tag{20}$$

The error minimization results in three decoupled component optimization problems defined in the following.

The compressor component optimization selects prescribed values $\tilde{\mathbf{p}}_C^s$ for the shared design variables relevant for the compressor, the coupling quantities $\tilde{\mathbf{y}}_{i|j}$ for the compressor and the prescribed goal for the component efficiency $\tilde{\eta}_C$ from the global design vector (18) and summarizes them as

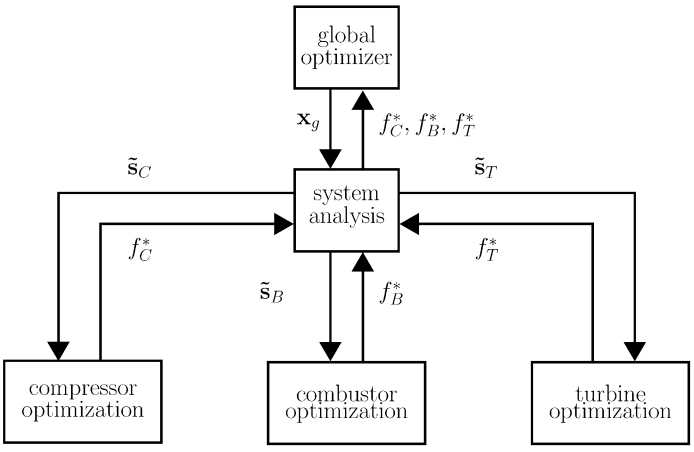

Figure 2 CO strategy

$$\tilde{\mathbf{s}}_C = \left[\tilde{\mathbf{p}}_C^{s^T}, \tilde{\mathbf{y}}_{C|B}^T, \tilde{\mathbf{y}}_{T|C}^T, \tilde{\mathbf{y}}_{C|T}^T, \tilde{\eta}_C\right]^T. \quad (21)$$

The design variables used on component-level for optimization are local design variables $\mathbf{p}_C^l$, relevant shared design variables $\mathbf{p}_C^s$ and coupling input $\mathbf{y}_{T|C}$ from the turbine component. They are summarized in the design vector

$$\mathbf{x}_C = \left[\mathbf{p}_C^{l^T}, \mathbf{p}_C^{s^T}, \mathbf{y}_{T|C}^T\right]^T. \quad (22)$$

The local component analysis is performed using $\mathbf{x}_C$ as input and yields subsystem answers $\mathbf{y}_{C|B}, \mathbf{y}_{C|T}, \eta_C$ summarized as $\mathbf{s}_C(\mathbf{x}_C)$ similar to Eq. (21). The goal for the compressor optimization process is to minimize the deviation

$$f_C(\mathbf{x}_C) = \|\mathbf{s}_C(\mathbf{x}_C) - \tilde{\mathbf{s}}_C\|_2 \quad (23)$$

resulting in the component optimization problem

$$f_C^* = \min_{\mathbf{x}_C \in S_C} f_C(\mathbf{x}_C) \text{ where } S_C = \{\mathbf{x}_C \in \mathbb{R}^3 | \check{\mathbf{x}}_C \le \mathbf{x}_C \le \hat{\mathbf{x}}_C\}. \quad (24)$$

The optimal value f_C^* is then returned to the global optimizer according to Fig. 2.

The combustor subsystem uses a similar vector of prescribed values summarized as

$$\tilde{\mathbf{s}}_B = \left[\tilde{\mathbf{p}}_B^{s^T}, \tilde{\mathbf{y}}_{C|B}^T, \tilde{\mathbf{y}}_{B|T}^T, \tilde{\eta}_B\right]^T. \quad (25)$$

The set of design variables used during optimization is defined similar to (22) as

$$\mathbf{x}_B = \left[\mathbf{p}_B^{l^T}, \mathbf{p}_B^{s^T}, \mathbf{y}_{C|B}^T\right]^T, \quad (26)$$

and the combustor goal function is similar to (23):

$$f_B(\mathbf{x}_B) = \|\mathbf{s}_B(\mathbf{x}_B) - \tilde{\mathbf{s}}_B\|_2. \quad (27)$$

This results in the combustor optimization problem

$$f_B^* = \min_{\mathbf{x}_B \in S_B} f_B(\mathbf{x}_B) \text{ where } S_B = \{\mathbf{x}_B \in \mathbb{R}^8 | \check{\mathbf{x}}_B \le \mathbf{x}_B \le \hat{\mathbf{x}}_B\}. \quad (28)$$

The turbine subsystem formulation differs from the two mentioned component problems in that it needs to observe additionally the turbine exit coupling (15) as an inequality constraint to be fulfilled within a certain margin ε_T^l. This results in

$$f_T^* = \min_{\mathbf{x}_T \in S_T} f_T(\mathbf{x}_T) \text{ where } S_T = \left\{\mathbf{x}_T \in \mathbb{R}^6 \middle| \|\mathbf{y}_5 - \tilde{\mathbf{y}}_5\|_2 \le \varepsilon_T^l, \check{\mathbf{x}}_T \le \mathbf{x}_T \le \hat{\mathbf{x}}_T\right\}. \quad (29)$$

The values prescribed by the global optimizer are

$$\tilde{\mathbf{s}}_T = \left[\tilde{\mathbf{p}}_T^{s^T}, \tilde{\mathbf{y}}_{B|T}^T, \tilde{\mathbf{y}}_{T|C}^T, \tilde{\mathbf{y}}_{C|T}^T, \tilde{\eta}_T\right]^T, \quad (30)$$

the design vector of the subprocess is

$$\mathbf{x}_T = \left[\mathbf{p}_T^{l^T}, \mathbf{p}_T^{s^T}, \mathbf{y}_{C|T}^T, \mathbf{y}_{B|T}^T\right]^T, \quad (31)$$

and the objective is

$$f_T(\mathbf{x}_T) = \|\mathbf{s}_T(\mathbf{x}_T) - \tilde{\mathbf{s}}_T\|_2. \quad (32)$$

BLISS 2000

The second cascaded optimization scheme called BLISS 2000 is a proposal by Sobieszczanski-Sobieski et al. (2003). In addition to the prescribed interface states $\mathbf{y}_{i|j}$ and global design variables $\mathbf{p}^s$, weights for local outputs are provided. These values define the system state and are summarized in global design vector

$$\mathbf{x}_g = \left[\mathbf{p}^{s^T}, \tilde{\mathbf{y}}_{C|B}^T, \mathbf{w}_{C|B}^T, \tilde{\mathbf{y}}_{C|T}^T, \mathbf{w}_{C|T}^T, \tilde{\mathbf{y}}_{B|T}^T, \mathbf{w}_{B|T}^T, \tilde{\mathbf{y}}_{T|C}^T, \mathbf{w}_{T|C}^T, w_{\eta,C}, w_{\eta,B}, w_{\eta,T}\right]^T. \quad (33)$$

The structure of the cascaded process provided in Fig. 3 is rather similar to that of the CO process where here the overall engine efficiency (16) is calculated from the returned component efficiencies. This is then used in the overall optimization problem

$$\max_{\mathbf{x}_g \in S} \eta\left(\mathbf{x}_g\right) \text{ where } S = \left\{\mathbf{x}_g \in \mathbb{R}^{20} \middle| \begin{bmatrix} h_C \\ h_B \\ h_T \end{bmatrix} \le \begin{bmatrix} \varepsilon_C \\ \varepsilon_B \\ \varepsilon_T \end{bmatrix}, \check{\mathbf{x}}_g \le \mathbf{x}_g \le \hat{\mathbf{x}}_g\right\}. \quad (34)$$

While optimizing the overall efficiency, the BLISS 2000 method also observes inequality constraints for the system coupling consistency by comparing calculated values $\mathbf{y}_{i|j}^*$ for coupling quantities with the values $\tilde{\mathbf{y}}_{i|j}$ prescribed by the global optimizer. The identities have to be fulfilled within certain tolerances ε_i resulting in constraint functions

$$h_C = \left\| \begin{bmatrix} \mathbf{y}_{C|B}^*\left(\mathbf{p}_C^l, \mathbf{p}_C^s, \tilde{\mathbf{y}}_{T|C}\right) - \tilde{\mathbf{y}}_{C|B} \\ \mathbf{y}_{C|T}^*\left(\mathbf{p}_C^l, \mathbf{p}_C^s, \tilde{\mathbf{y}}_{T|C}\right) - \tilde{\mathbf{y}}_{C|T} \end{bmatrix} \right\|_2,$$
$$h_B = \left\| \left[\mathbf{y}_{B|T}^*\left(\mathbf{p}_B^l, \mathbf{p}_B^s, \tilde{\mathbf{y}}_{C|B}\right) - \tilde{\mathbf{y}}_{B|T}\right] \right\|_2, \quad (35)$$
$$h_T = \left\| \left[\mathbf{y}_{T|C}^*\left(\mathbf{p}_T^l, \mathbf{p}_T^s, \tilde{\mathbf{y}}_{C|T}\right) - \tilde{\mathbf{y}}_{T|C}\right] \right\|_2.$$

The compressor component optimization uses a goal function where not only the component efficiency η_C is maximized, but also the outputs. The contribution of these terms may be influenced by weights prescribed by the global optimizer and fixed during subsystem optimization. This leads to the goal function

$$f_C = \mathbf{w}_{C|B}^T \tilde{\mathbf{y}}_{C|B} + \mathbf{w}_{C|T}^T \tilde{\mathbf{y}}_{C|T} + w_{\eta,C}\eta_C \quad (36)$$

to be maximized by varying local design variables only. This results in an unconstrained optimization problem

$$\max_{\mathbf{p}_C^l \in C} f_C \text{ where } C = \left\{\mathbf{p}_C^l \in \mathbb{R} \middle| \check{\mathbf{p}}_C^l \le \mathbf{p}_C^l \le \hat{\mathbf{p}}_C^l\right\}. \quad (37)$$

Similarly, the combustor optimization problem reads as

$$\max_{\mathbf{p}_B^l \in B} f_B \text{ where } B = \left\{\mathbf{p}_B^l \in \mathbb{R}^2 \middle| \check{\mathbf{p}}_B^l \le \mathbf{p}_B^l \le \hat{\mathbf{p}}_B^l\right\}, \quad (38)$$

using local design variables (8) to achieve a maximal value for the weighted goal function

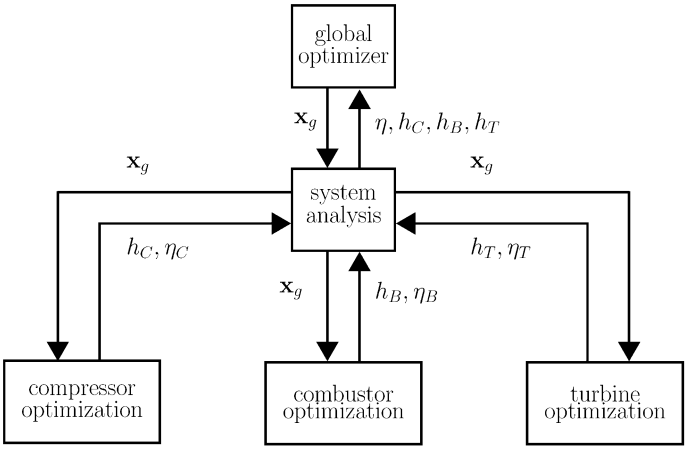

Figure 3 BLISS 2000 optimization strategy

$$f_B = \mathbf{w}_{B|T}^T \tilde{\mathbf{y}}_{B|T} + w_{\eta,B}\eta_B. \tag{39}$$

Finally, turbine optimization is defined as a constrained optimization problem

$$\max_{\mathbf{p}_T^l \in T} f_T \text{ where}$$
$$T = \left\{\mathbf{p}_T^l \in \mathbb{R} \middle| \|\mathbf{y}_5 - \tilde{\mathbf{y}}_5\|_2 \le \varepsilon_T^l, \check{\mathbf{p}}_T^l \le \mathbf{p}_T^l \le \hat{\mathbf{p}}_T^l\right\} \tag{40}$$

using local design vector (13) and the turbine compliance as a local constraint besides maximizing the objective

$$f_T = \mathbf{w}_{T|C}^T \mathbf{y}_{T|C} + w_{\eta,T}\eta_T. \tag{41}$$

ISOC Strategy

The third cascaded strategy is the Interface Segmentation Optimization Concept (ISOC) proposed by Lockan et al. (2017), which assesses the approximation of optimal performance and feasible regions in the interface space between coupled components. The goal of the decoupled local optimizations is to improve these approximations. The interface approximations define the feasible space of configurations and within these limits the search for an optimal configuration is performed. The problem is solved iteratively with a trust region approach searching for valid and possibly optimal configurations for the coupled core engine. In Fig. 4 the layout of the optimization strategy is provided, where the global optimizer modifies the system design vector

$$\mathbf{x}_g = \left[\mathbf{p}^{s^T}, \mathbf{y}_{C|B}^T, \mathbf{y}_{C|T}^T, \mathbf{y}_{B|T}^T, \mathbf{y}_{T|C}^T\right]^T \tag{42}$$

for the whole optimization problem containing shared design variables $\mathbf{p}^s$ as well as coupling vectors $\mathbf{y}_{i|j}$. The goal is to reach an optimal overall efficiency (16) subject to constraints on the quality of the interface approximations F_i, where errors have to stay below certain thresholds ε_i:

$$\max_{\mathbf{x}_g \in S} \eta \text{ where}$$
$$S = \left\{\mathbf{x}_g \in \mathbb{R}^{10} \middle| \begin{bmatrix} F_C \\ F_B \\ F_T \end{bmatrix} \le \begin{bmatrix} \varepsilon_C \\ \varepsilon_B \\ \varepsilon_T \end{bmatrix}, \check{\mathbf{x}}_g \le \mathbf{x}_g \le \hat{\mathbf{x}}_g\right\}. \tag{43}$$

Optimization is performed solely using approximations. In order to optimize the system in a decoupled manner reaching locally optimal results, which are also globally feasible and optimal, it is important to share information about feasibility and optimality between the components. This is done for the compressor via the two vectors

$$\mathbf{s}_{C|B} = \left[\mathbf{p}_{C\&B}^{s^T}, \mathbf{y}_{C|B}^T(\mathbf{p}_C)\right]^T,$$
$$\mathbf{s}_{C|T} = \left[\mathbf{p}_{C\&T}^{s^T}, \mathbf{y}_{C|T}^T(\mathbf{p}_C), \tilde{\mathbf{y}}_{T|C}^T\right]^T \tag{44}$$

containing shared design variables for compressor and combustor, and compressor and turbine, respectively. The design variables $\mathbf{p}_{C\&B}^s$ are used by either component and the coupling vector $\mathbf{y}_{C|B}(\mathbf{p}_C)$ is calculated as a function of compressor design variables $\mathbf{p}_C$. The performance of the compressor can also be calculated directly as $\eta_C(\mathbf{p}_C)$, whereas efficiencies $\eta_B^*(\mathbf{s}_{C|B})$ and $\eta_T^*(\mathbf{s}_{C|T})$ for combustor and turbine are estimated from approximations defined on the interface spaces. The estimation of interface behaviour is presented in detail by Lockan (2017). The component efficiencies then result in an estimated overall efficiency

$$\eta = \eta_C(\mathbf{p}_C)\eta_B^*(\mathbf{s}_{C|B})\eta_T^*(\mathbf{s}_{C|T}). \tag{45}$$

An important point during the optimization is to determine whether or not the given configuration is valid.

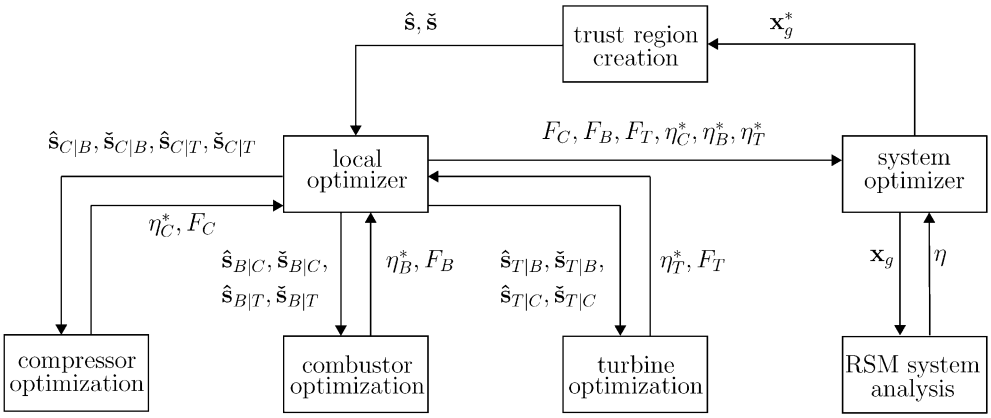

Figure 4 ISOC optimization strategy

Thus, a probability of feasibility $F_{B|C}$ and $F_{T|C}$ is assigned to vectors $\mathbf{s}_{C|B}$ and $\mathbf{s}_{C|T}$ for each interface subject. The probability has to stay below certain values $\varepsilon_{B|C}$ and $\varepsilon_{T|C}$ which represent the approximation error derived from a cross validation. These probabilities of feasibility determine the space of valid solutions in which an optimum for the local optimization problem

$$\max_{\mathbf{p}_C \in P_C} \eta \text{ where}$$

$$P_C = \left\{ \mathbf{p}_C \in \mathbb{R}^2 \left| \begin{bmatrix} F_{B|C}(\mathbf{s}_{C|B}) \\ F_{T|C}(\mathbf{s}_{C|T}) \end{bmatrix} \leq \begin{bmatrix} \varepsilon_{B|C} \\ \varepsilon_{T|C} \end{bmatrix}, \breve{\mathbf{p}}_C \leq \mathbf{p}_C \leq \hat{\mathbf{p}}_C \right. \right\} \tag{46}$$

needs to be found.

The combustor optimization problem is defined similarly with interface vectors

$$\begin{aligned} \mathbf{s}_{B|C} &= \left[\mathbf{p}_{B\&C}^{s^T}, \tilde{\mathbf{y}}_{C|B}^T \right]^T, \\ \mathbf{s}_{B|T} &= \left[\mathbf{p}_{B\&T}^{s^T}, \mathbf{y}_{B|T}^T(\mathbf{p}_B) \right]^T \end{aligned} \tag{47}$$

between combustor and the other two subsystems. The component optimization problem is then

$$\max_{\mathbf{p}_B \in P_B} \eta \quad \text{where}$$

$$P_B = \left\{ \mathbf{p}_B \in \mathbb{R}^5 \left| \begin{bmatrix} F_{C|B}(\mathbf{s}_{B|C}) \\ F_{T|B}(\mathbf{s}_{B|T}) \end{bmatrix} \leq \begin{bmatrix} \varepsilon_{C|B} \\ \varepsilon_{T|B} \end{bmatrix}, \breve{\mathbf{p}}_B \leq \mathbf{p}_B \leq \hat{\mathbf{p}}_B \right. \right\}. \tag{48}$$

The local efficiency estimate now results from a direct efficiency calculating $\eta_B(\mathbf{p}_B)$ for the combustor and estimates for compressor and turbine:

$$\eta = \eta_C^*(\mathbf{s}_{B|C}) \eta_B(\mathbf{p}_B) \eta_T^*(\mathbf{s}_{B|T}). \tag{49}$$

In principle, the turbine subprocess is similar, but additionally takes into account turbine exit $\mathbf{y}_5$ as constraint:

$$\max_{\mathbf{p}_T \in P_T} \eta \quad \text{where}$$

$$P_T = \left\{ \mathbf{p}_T \in \mathbb{R}^3 \left| \begin{bmatrix} F_{C|T}(\mathbf{s}_{T|C}) \\ F_{B|T}(\mathbf{s}_{T|B}) \\ \|\mathbf{y}_5 - \tilde{\mathbf{y}}_5\|_2 \end{bmatrix} \leq \begin{bmatrix} \varepsilon_{C|T} \\ \varepsilon_{B|\mathrm{T}} \\ \varepsilon_T^l \end{bmatrix}, \breve{\mathbf{p}}_T \leq \mathbf{p}_T \leq \hat{\mathbf{p}}_T \right. \right\}. \tag{50}$$

Interface representations are

$$\begin{aligned} \mathbf{s}_{T|B} &= \left[\mathbf{p}_{T\&B}^{s^T}, \tilde{\mathbf{y}}_{B|T}^T \right]^T, \\ \mathbf{s}_{T|C} &= \left[\mathbf{p}_{T\&C}^{s^T}, \tilde{\mathbf{y}}_{T|C}^T(\mathbf{p}_T), \tilde{\mathbf{y}}_{C|T}^T \right]^T, \end{aligned} \tag{51}$$

and the overall efficiency is estimated as

$$\eta = \eta_C^*(\mathbf{s}_{T|C}) \eta_B^*(\mathbf{s}_{T|B}) \eta_T(\mathbf{p}_T). \tag{52}$$

APPLICATION TO THE THERMODYNAMIC MODEL

Each optimization approach is applied to the thermodynamic model for decoupled core engine optimization and iterated until convergence or a prescribed limit of iterations is reached. The prescribed limit here is the amount of global iterations, whereas the amount of component evaluations is used as a performance metric. The reference AAO optimization is stopped when no further improvement is made. The performance of the different strategies is judged by their ability to reach an improvement over the reference design with a certain number of iterations. Global and local iterations are treated separately, because they have a different impact on the overall wall clock time.

For statistical evaluation, all four algorithms are executed ten times. Each optimization starts with the same reference configuration derived from an industrial application example. The same constraints and tolerances are applied to all optimizations. The results for all four methods are shown in Fig. 5, where the mean relative efficiency $\bar{\eta}_{norm}$ is normalized with respect to the results of the AAO and plotted against the number $\bar{n}_{local}$ of any of the incorporated subsystem evaluations. The data in Fig. 6 represents the scalability of the methods, showing an overall optimization runtime estimate $\bar{t}_{global}$ over the computation time t_{local} for a single component analysis. It is extrapolated from the best efficiency point of the AAO reference, marked by the horizontal line in Fig. 5. Only the wall clock time of the component analyses are scaled, not the time of the method itself, which is independent from component runtimes.

The results for the AAO reference optimization are obtained using a genetic algorithm (GA) as the sole optimizer required in this strategy. The method reaches its optimal solution after a mean of 18493 subsystem evaluations, Fig. 5. The wall clock time of 9h to reach this result is longer than the 4.2min required by CO to reach a comparable efficiency, and overall runtime of 2.5h for obtaining its final best value. The improvement in core engine efficiency found by AAO is less than that of all other methods. According to Fig. 6 AAO scales worse than the ISOC method due to the high number of function evaluations needed to find a consistent system state in every iteration loop. This has a substantial impact on performance for longer-running component analyses, i.e. when higher-fidelity analyses are used.

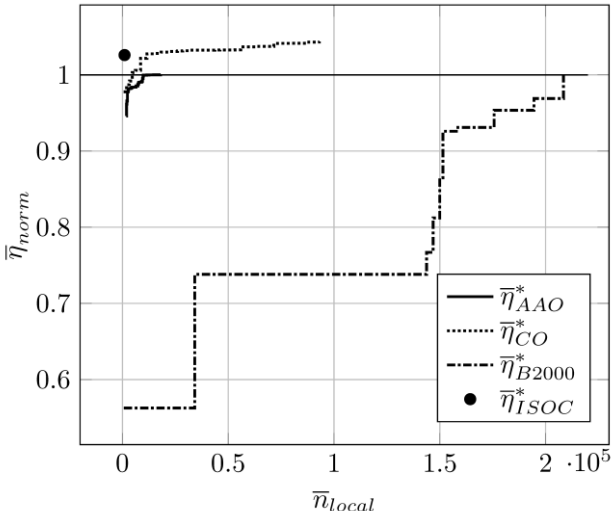

Figure 5 Mean normalized core engine fitness function

The first cascaded method presented in this paper, the CO, uses on system level an efficient global optimizer called MSRS (Multistart Stochastical Response Surface) by Regis and Shoemaker (2007). It is based on approximations by response surfaces reducing the number of direct design evaluations. That makes it well suited, because one of the most important aspects of cascaded methods is a low number of global system evaluations. The local optimizations are performed using the same GA as for AAO, because the low number of local variables and short running times do not negatively affect the performance of the GA, keeping it as a viable option. The CO method shows the best performance regarding the quality of the optimization result. In the mean of all test runs it achieves the highest improvement in core engine efficiency. It also achieves a very low wall clock time, which seems contradictory to the data in Fig. 5. Due to the structure of the CO method, it is very well suited for parallelization. Thus, it can perform more calculations on the component level for a given time than the AAO approach, explaining the discrepancy between the data in Fig. 5 and the

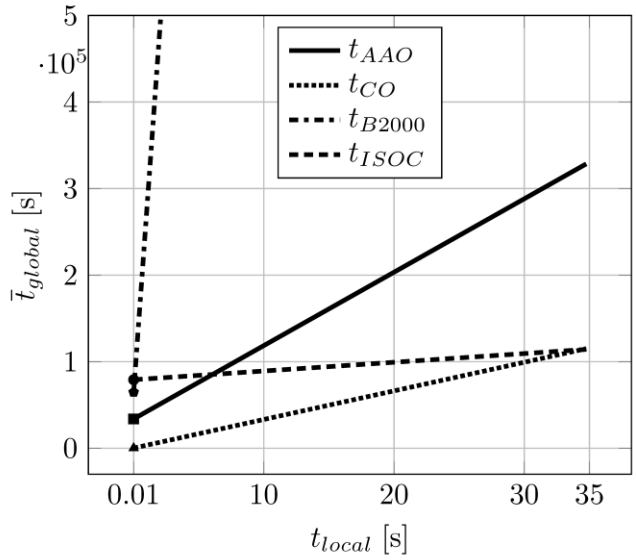

Figure 6 Overall optimization runtimes over component analysis runtimes

actual run times. Its performance scaling for longer running component processes shown in Fig. 6, however, is quite low. The high amount of subsystem evaluations with a mean number of 2043 per local optimization step (equal to one global iteration) leads to a longer runtime. This may be countered to a certain degree by using further parallelization, but will not solve the problem at its core. Another downside to CO is that not only the coupling vectors need to be prescribed, but also goals $\tilde{\eta}_C, \tilde{\eta}_B$ and $\tilde{\eta}_T$ for component performances are required. Thus, the user needs a good understanding of the expected component performance beforehand to prescribe suited ranges for optimization. If ranges are set too wide, substantial computation time is wasted on invalid configurations, if they are set too narrow, the design space is too restricted. Therefore, a sensitivity analysis may be performed to reduce this disadvantage.

The BLISS 2000 global optimization is also performed using the MSRS algorithm for global and GA for local optimization. The BLISS 2000 method performs slightly better than AAO with regards to maximum efficiency, but performs worse than both CO and ISOC. The BLISS 2000 requires more subsystem evaluations to find a consistent system state. This is due to the enlarged design space for the overall optimization problem which is inflated by the weights provided for coupling vectors and component goal functions. This inflation in design space compared to CO is compensated in part by smaller local design spaces. The overall number of system evaluations needed is still greater, because the drop in local evaluations does not fully compensate the increase in computational load on the system analysis process, compared to the CO. Furthermore, the weights are not limited to a range $w_i \in [0,1]$, which makes it difficult to set ranges allowing for stable convergence. The number of weights rises with the dimension of coupling vectors and design goals for the components, which leads to a high-dimensional overall design space. This in turn requires a higher number of samples in a DoE and more iterations to converge to a valid solution. In addition to the inflated design space, the BLISS 2000 for non-convex problems is not guaranteed to converge to the optimal solution of the problem. This, together with the higher number of optimization variables explains the worse performance compared to the other methods shown here. It scales worse than the other methods due to the required initial computation time.

The ISOC-based optimization is performed using the MSRS algorithm for local optimizations, while the system optimization is performed with a GA. This is because the system optimization is based on response surfaces, and thus a less efficient algorithm does not increase the overall runtime. The system optimization is coordinated by a trust region approach. The results for the core engine efficiency are represented by a single marker in Fig. 5, because the ISOC method does not provide consistent system states during optimization. If there is a possible consistent system state to be found for the given problem, it will be provided as the result at the end of the processes run only. That may pose a challenge in certain engineering applications, i.e., for

concurrent design work on a single project, where different departments require an updated version of the currently best design. For the present example, the ISOC yields a good result considering the very low mean number of 933 subsystem evaluations. This comes at the cost of a slightly higher runtime of 22h, which is due to the need to create response surfaces. The low number of subsystem evaluations leads to a very robust result for scalability. The ISOC has the lowest impact of subsystem calculation time on the overall computation time of all the algorithms compared here, and thus is best suited for the cascaded optimization of complex component analyses.

CONCLUSIONS

The cascaded methods presented in this paper show a high level of optimization performance for the given problem emulating a complex core engine optimization problem. It is shown that they achieve a good performance regarding improvement over the baseline configuration and a short runtime in the case of the CO. The ISOC performs well for the given problem and is supposed to have the highest performance when using more complex component analysis tools. The results presented in this paper will be applied to a more complex optimization problem in the future to validate the findings and create an effective tool for preliminary core engine design.

NOMENCLATURE

$\mathbf{h}$	constraint vector
$\mathbf{p}$	design vector
$\mathbf{s}$	system design vector
$\mathbf{y}$	coupling vector
α	bleed air fraction
β	fuel-to-air-ratio (FAR)
η	efficiency
ε	tolerance
κ	ratio of specific heats
π	pressure ratio
A	flow area
c_p	specific heat capacity
f	objective function
F	approximation quality
H_u	specific heating value
$\dot{m}$	mass flow
n	number of iterations
p_t	total pressure
T_t	total temperature
$\widetilde{\bullet}$	prescribed value
$\check{\bullet}, \hat{\bullet}$	lower bound, upper bound
$\overline{\bullet}$	mean value
$\bullet^*$	optimal value

ACKNOWLEDGMENTS

This work has been carried out in collaboration with Rolls-Royce Deutschland as part of the research project VITIV (Virtual Turbomachinery Design with Integrative Strategies, Proj.-No. 80164702) funded by the State of Brandenburg, the European Regional Development Fund, and Rolls-Royce Deutschland. Rolls-Royce Deutschland's permission to publish this work is greatly acknowledged.

REFERENCES

Braun, R.D., Kroo, I.M. (1995). Development and Application of the Collaborative Optimization Architecture in a Multidisciplinary Design Environment. NASA Langley Technical Report, Hampton.

Bräunling, W.J.G. (2009). Flugzeugtriebwerke: Grundlagen, Aero-Thermodynamik, ideale und reale Kreisprozesse, Thermische Turbomaschinen, Komponenten, Emissionen und Systeme. Springer, Berlin.

Cramer, E.J., Dennis, J.E., Frank, P.D., Lewis, R.M., and Shubin, G.R. (1994). Problem Formulation for Multidisciplinary Optimization. SIAM Journal on Optimization 4, pp. 754–776.

Extra, S., Lockan, M., Bestle, D., and Flassig, P. (2017). Coupled Subsystem Optimization for Preliminary Core Engine Design. Proc. of ECCOMAS EUROGEN, Madrid, to be published in 2018.

Kupijai, P. (2014). Ein Beitrag zur automatisierten Triebwerksvorauslegung. Dissertation, Shaker, Aachen.

Lockan, M. (2017). Kooperative Optimierung komplexer Systeme durch Segmentierung des Interface-Raums. Dissertation, Shaker, Aachen.

Lockan, M., Bestle, D., Janke, C., Meyer, M. (2017). Optimization of Coupled System Components Using Approximations of Interface Quantities. Proc. of ASME Turbo Expo, Charlotte, GT2017-64135.

Regis, R.G., Shoemaker, C.A. (2007). A Stochastic Radial Basis Function Method for the Global Optimization of Expensive Functions. INFORMS Journal on Computing 19(4), pp. 497–509.

Sobieszczanski-Sobieski, J. (1984). Optimization by Decomposition: A Step from Hierarchic to Non-hierarchic Systems. NASA Langley Research Center, Hampton.

Sobieszczanski-Sobieski, J., Altus, T.D., Phillips, M., and Sandusky R. (2003). Bilevel Integrated System Synthesis for Concurrent and Distributed Processing. AIAA Journal 41, pp. 1996–2003.